Electronic Supplementary Material (ESI) for ChemComm.

Polymer-Induced Polymorphism in a Zn-Based Metal Organic Framework

Supporting Information

Karl S. Westendorff,[†] Christopher Paolucci,[*, †] and Gaurav Giri[*, †]

†Department of Chemical Engineering, University of Virginia, Charlottesville, VA 22903 (USA)

E-mail: gg3qd@virginia.edu, cp9wx@virginia.edu

Contents

Synthetic/Analytical Methodology and Results

Synthesis of ZIF MOFs

All chemicals ($Zn(NO_3)_2•6H_2O$, 2-methylimidazole, and 100,000 MW PEO) were obtained from Sigma Aldrich and were used without further modification. All ZIF-8/ZIF-L MOF variations were synthesized at room temperature and atmospheric pressure. In a typical synthesis, 2.27 g of 2-methylimidazole was dissolved in 20 mL of DI water while varying amounts of $Zn(NO_3)_2•6H_2O$ were dissolved in a separate 10 mL of DI water. 100,000 MW PEO was added to 10 mL of DI water such that it was 0.5 wt% of all component solutions. All solutions were stirred until complete dissolution, after which the polymer and ligand solutions were combined and then added to the metal solution. The total mixtures were left to stir for 4 hours. The resulting solutions were centrifuged, washed with DI water, and dried before being characterized.

PXRD Parameters

XRD patterns were recorded on a PANalytical Empyrean X-ray diffractometer with a Cu K-α beam (λ = 1.54 Å). Scans were completed from a 2θ of 6° to 47.5° (Q range 0.36 Å-1 to 2.25 Å-1) with a step size of 0.0017°.

SEM Parameters

SEM images were collected with a FEI Quanta 650 at 3 kV with a spot size of 4 at various magnifications.

ZIF-8/ZIF-L Peak Identification

To confirm the successful synthesis of ZIF-8 and ZIF-L, PXRD patterns were compared to those calculated in Mercury. Experimental and calculated PXRD patterns are displayed along with the first several notable peaks listed by their <h,l,k> indices in **Figure S1** and **Figure S2** below.

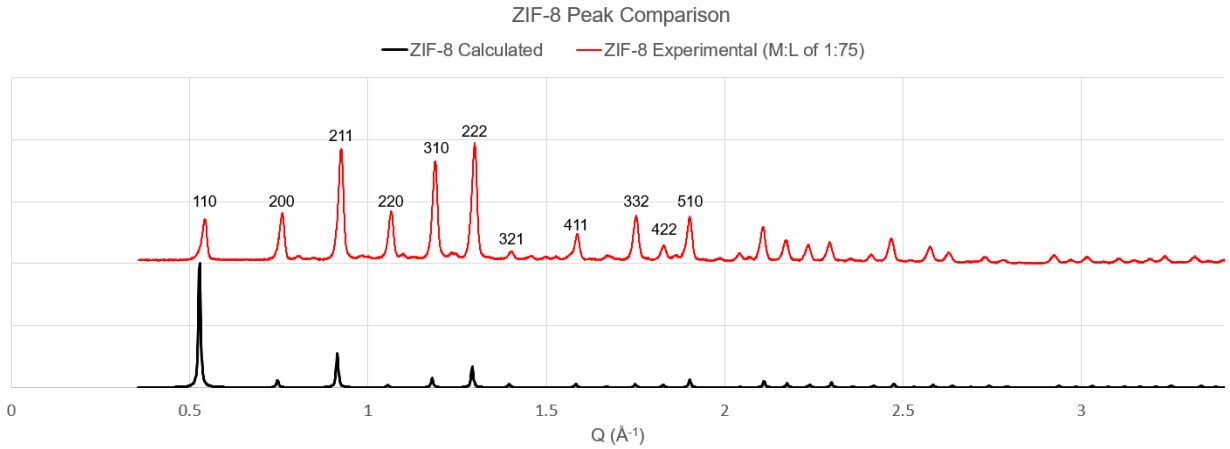

Figure S1. Experimental ZIF-8 (M:L of 1:75, red) and calculated ZIF-8 (black) patterns.

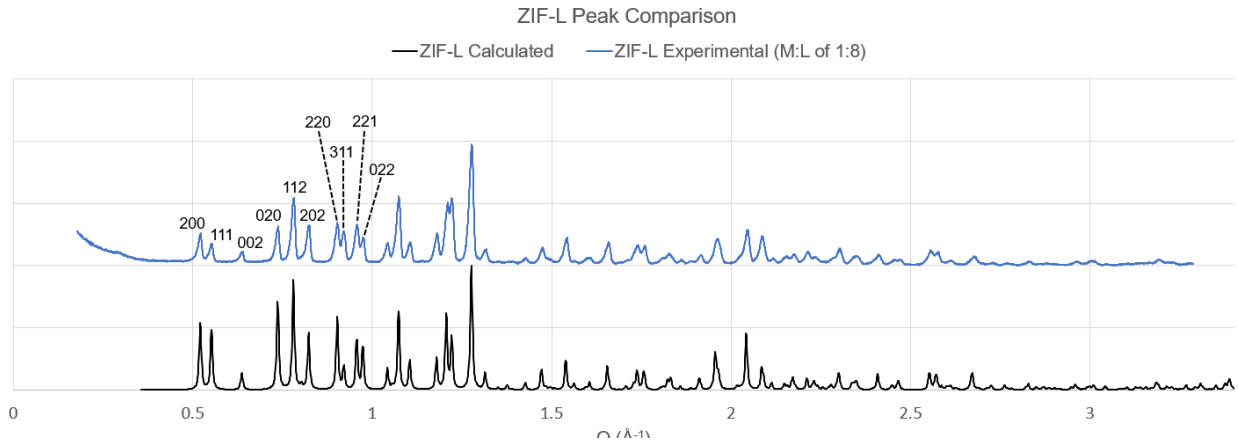

Figure S2. Experimental ZIF-L (M:L of 1:8, blue) and calculated ZIF-L (black) patterns.

Particle Sizes of ZIF with PEO Addition

Table S1. Measured particle diameters of ZIF crystals with and without the use of PEO during synthesis. ImageJ was used to analyze distances in the SEMs featured in Figure 2.

M:L ratio	Without PEO Particle Diameter (μm)	With PEO Particle Diameter (μm)
4	2.39 ± 1.84	0.86 ± 0.17
8	2.46 ± 0.53	0.61 ± 0.11
12	1.64 ± 0.23	0.50 ± 0.14
16	2.32 ± 0.52	0.53 ± 0.06
25	2.17 ± 0.18	0.39 ± 0.07
41	1.88 ± 0.17	0.41 ± 0.06
58	1.77 ± 0.40	0.44 ± 0.06
75	1.65 ± 0.15	0.20 ± 0.03

Computational Methodology and Results

Creation of Periodic Models

Periodic DFT calculations were carried out in the Vienna ab initio Simulation Package (VASP), version 5.4.4.[1] Crystal structures obtained from Morris et al. and Chen et al. were used as initial guesses for ZIF-8 and ZIF-L structures, respectively, in these calculations.[2,3] Geometry optimizations were completed by applying the Perdew-Becke-Ernzerhof (PBE) generalized gradient approximation (GGA) exchange-correlation functional coupled with Becke-Johnson damping (D3(BJ)vdw) dispersion correction method.[4-6] An energy cutoff of 400 eV was used, and we only considered Γ point for sampling the first Brillouin zone. Convergence criteria of 10^{-6} eV and 0.03 eV/Å were used for self-consistent-field (SCF) electronic energies and atomic forces, respectively.

Creation of Cluster Models

Starting with the PBE-optimized periodic geometries of ZIF-8 and ZIF-L, we created cluster models in the same manner as Chizallet et al, with a single Zn(II) atom surrounded by deprotonated 2-methylimidazole ligands, and a single protonated 2-methylimidazole ligand in the case of ZIF-L.[7,8] In all subsequent calculations, the appropriate overall charge was utilized and we froze the atomic positions of these clusters. In PEO-coordinated structures, we positioned the abridged chains to form four-coordinated complexes and optimized the PEO chains. We then performed frequency calculations to obtain Gibbs free energies. All calculations were performed utilizing Gaussian 16 at the B3LYP level of theory with GD3BJ empirical dispersion corrections, using the default Gaussian convergence criteria (max force < $4.5*10^{-4}$, RMS force < $3*10^{-4}$, max displacement < $1.8*10^{-3}$, RMS displacement < $1.2*10^{-3}$, all criteria in atomic units).[9,10,6] All calculations were performed using the def2-TZVPP basis set.[11,12] All structures utilized in this work are included in an attached series of .xyz files (structures.zip). A summary of the clusters is shown in **Figure S3**.

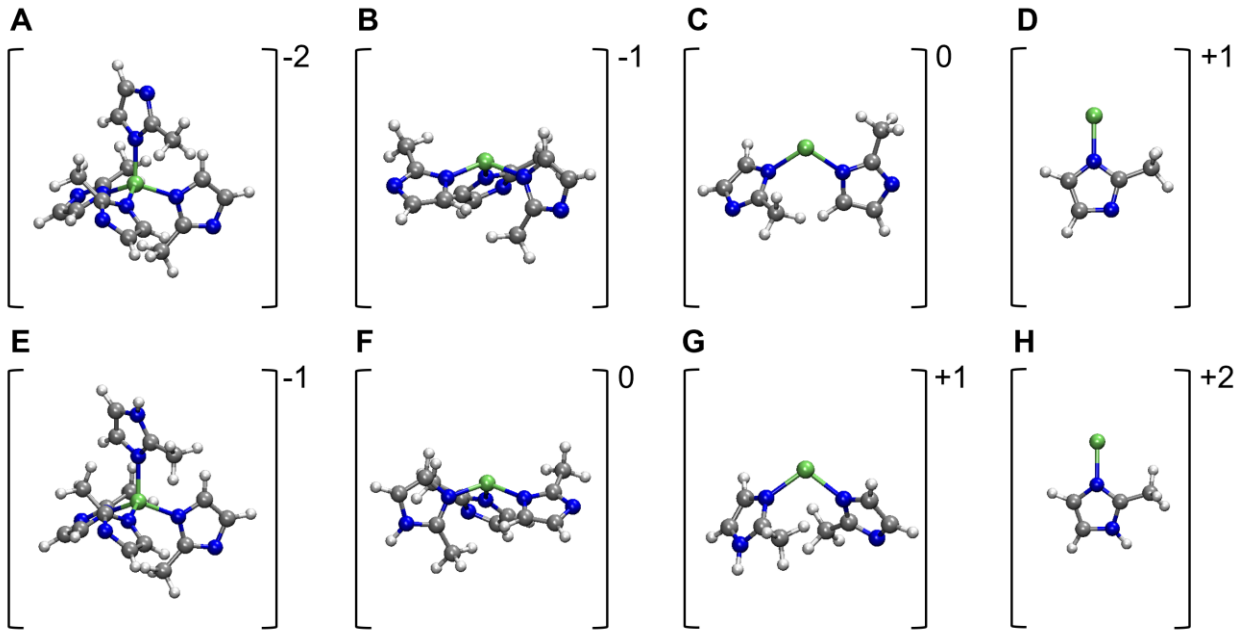

Figure S3. ZIF-8 (A-D) and ZIF-L (E-H) cluster models. All Zn centers are of a 2+ oxidation state and appropriate charge balances are applied on the structure, noting that deprotonated 2-methylimidazole ligands have a -1 charge and that protonated 2-methylimidazole ligands are neutral. Zinc atoms are shown in green, nitrogen in blue, carbon in grey, and hydrogen in white.

Reactions Modelled

We computed PEO binding energies according to eqs S1 and S2. Here, *n* is the number of ligands bound to the Zn metal center.

$$[\text{ZIF8-n}]^{+2-n} + \text{PEO} \xrightarrow{\Delta G^{\circ}_{\text{ZIF8}}} [\text{ZIF8-n-PEO}]^{+2-n} \quad \text{(S1)}$$

$$[\text{ZIFL-n}]^{+3-n} + \text{PEO} \xrightarrow{\Delta G^{\circ}_{\text{ZIFL}}} [\text{ZIFL-n-PEO}]^{+3-n} \quad \text{(S2)}$$

Structure Free Energies and Zn Mulliken Charges

Table S2. Calculated Gibbs free energies (1 M, 298 K) and Zn atom Mulliken charges. PEO 5 and PEO 7 denote polyethylene oxide chains with 5 and 7 monomer units, respectively. Chains were terminated with methyl and hydroxyl groups at either end. ZIF8-n and ZIFL-n labels denote the number (n) of 2-methylimidazole ligands bound to the complex.

Species	Gibbs Free Energies (kJ/mol)	Zn atom Mulliken Charges (a.u)
PEO 5	-2022867	N/A
PEO 7	-2830737	N/A
ZIF8-1	-5366831	0.593
ZIF8-1-PEO5	-7390053	0.513
ZIF8-1-PEO7	-8197925	0.512
ZIFL-1	-5367380	0.973
ZIFL-1-PEO5	-7390865	0.595
ZIFL-1-PEO7	-8198738	0.601
ZIF8-2	-6063351	0.357
ZIF8-2-PEO5	-8086359	0.412
ZIF8-2-PEO7	-8894226	0.409
ZIFL-2	-6064347	0.462
ZIFL-2-PEO5	-8087437	0.528
ZIFL-2-PEO7	-8895305	0.526
ZIF8-3	-6759485	0.331
ZIF8-3-PEO5	-8782397	0.559
ZIF8-3-PEO7	-9590270	0.562
ZIFL-3	-6760789	0.304
ZIFL-3-PEO5	-8783709	0.657
ZIFL-3-PEO7	-9591576	0.654

Convergence of Polymer Coordination Reaction Energies

To determine the acceptable size of polymer modelled, 5 and 7 monomer structures were used. By examining the agreement of Zn Mulliken charges and convergence of reaction energies, we determined that 5 monomer polymer structures were sufficient to obtain reaction energies.

Table S3. Reaction energies for 5 and 7 monomer polymer chains at 1 atm and 298 K. Reaction energies calculated per eqs S1 and S2 for ZIF-8 and ZIF-L, respectively.

Reaction	Gibbs Free Energy of Reaction (kJ/mol)
$\text{ZIF8-1} + \text{PEO5} \xrightarrow{\Delta G^{\circ}_{\text{ZIF8}}} \text{ZIF8-1-PEO5}$	-355
$\text{ZIF8-1} + \text{PEO7} \xrightarrow{\Delta G^{\circ}_{\text{ZIF8}}} \text{ZIF8-1-PEO7}$	-356
$\text{ZIFL-1} + \text{PEO5} \xrightarrow{\Delta G^{\circ}_{\text{ZIFL}}} \text{ZIFL-1-PEO5}$	-618
$\text{ZIFL-1} + \text{PEO7} \xrightarrow{\Delta G^{\circ}_{\text{ZIFL}}} \text{ZIFL-1-PEO7}$	-621
$\text{ZIF8-2} + \text{PEO5} \xrightarrow{\Delta G^{\circ}_{\text{ZIF8}}} \text{ZIF8-2-PEO5}$	-141
$\text{ZIF8-2} + \text{PEO7} \xrightarrow{\Delta G^{\circ}_{\text{ZIF8}}} \text{ZIF8-2-PEO7}$	-138
$\text{ZIFL-2} + \text{PEO5} \xrightarrow{\Delta G^{\circ}_{\text{ZIFL}}} \text{ZIFL-2-PEO5}$	-223
$\text{ZIFL-2} + \text{PEO7} \xrightarrow{\Delta G^{\circ}_{\text{ZIFL}}} \text{ZIFL-2-PEO7}$	-220
$\text{ZIF8-3} + \text{PEO5} \xrightarrow{\Delta G^{\circ}_{\text{ZIF8}}} \text{ZIF8-3-PEO5}$	-44
$\text{ZIF8-3} + \text{PEO7} \xrightarrow{\Delta G^{\circ}_{\text{ZIF8}}} \text{ZIF8-3-PEO7}$	-47
$\text{ZIFL-3} + \text{PEO5} \xrightarrow{\Delta G^{\circ}_{\text{ZIFL}}} \text{ZIFL-3-PEO5}$	-53
$\text{ZIFL-3} + \text{PEO7} \xrightarrow{\Delta G^{\circ}_{\text{ZIFL}}} \text{ZIFL-3-PEO7}$	-50

Table S4. Difference in 7 monomer PEO binding energy between ZIF-L and ZIF-8 nodes. Gibbs free energies calculated at 1 M and 298 K.

# of Ligands	$\Delta G°_{ZIF8} - \Delta G°_{ZIFL}$ (kJ/mol)
1	265
2	82
3	3

Comparison of ZIF-8 and ZIF-L Binding Energies

The differences in PEO binding energies between ZIF-L and ZIF-8 nodes and proton transfer energies at every level of MOF formation are shown in **Table S5**. Positive energies indicate stronger binding to ZIF-L relative to ZIF-8.

Table S5. Difference in 5 monomer PEO binding energy between ZIF-L and ZIF-8 nodes. Gibbs free energies calculated at 1 M and 298 K. Positive energies indicate stronger binding to ZIF-L relative to ZIF-8.

# of Ligands	$\Delta G°_{ZIF8} - \Delta G°_{ZIFL}$ (kJ/mol)
1	263
2	82
3	8

References

(1) Kresse, G.; Furthmüller, J. Efficient Iterative Schemes for Ab Initio Total-Energy Calculations Using a Plane-Wave Basis Set. Phys. Rev. B 1996, 54 (16), 11169–11186.

(2) Chen, R.; Yao, J.; Gu, Q.; Smeets, S.; Baerlocher, C.; Gu, H.; Zhu, D.; Morris, W.; Yaghi, O. M.; Wang, H. A Two-Dimensional Zeolitic Imidazolate Framework with a Cushion-Shaped Cavity for CO2 Adsorption. *Chem. Commun.* **2013**, *49* (82), 9500–9502.

(3) Morris, W.; Stevens, C. J.; Taylor, R. E.; Dybowski, C.; Yaghi, O. M.; Garcia-Garibay, M. A. NMR and X-Ray Study Revealing the Rigidity of Zeolitic Imidazolate Frameworks. *J. Phys. Chem. C* **2012**, *116* (24), 13307–13312.

(4) Perdew, J. P.; Wang, Y. Accurate and Simple Analytic Representation of the Electron-Gas Correlation Energy. Phys. Rev. B 1992, 45 (23), 13244–13249.

(5) Grimme, S.; Antony, J.; Ehrlich, S.; Krieg, H. A Con-sistent and Accurate Ab Initio Parametrization of Density Functional Dispersion Correction (DFT-D) for the 94 El-ements H-Pu. J. Chem. Phys. 2010, 132 (15), 154104.

(6) Grimme, S.; Ehrlich, S.; Goerigk, L. Effect of the Damping Function in Dispersion Corrected Density Functional Theory. J. Comput. Chem. 2011, 32 (7), 1456–1465.

(7) Chizallet, C.; Bats, N. External Surface of Zeolite Imidazolate Frameworks Viewed Ab Initio: Multifunctionality at the Organic-Inorganic Interface. *J. Phys. Chem. Lett.* **2010**, *1* (1), 349–353.

(8) Chizallet, C.; Lazare, S.; Bazer-Bachi, D.; Bonnier, F.; Lecocq, V.; Soyer, E.; Quoineaud, A. A.; Bats, N. Catalysis of Transesterification by a Nonfunctionalized Metal-Organic Framework: Acido-Basicity at the External Surface of ZIF-8 Probed by FTIR and Ab Initio Calculations. *J. Am. Chem. Soc.* **2010**, *132* (35), 12365–12377.

(9) Frisch, M. J.; Trucks, G. W.; Schlegel, H. B.; Scuseria, G. E.; Robb, M. A.; Cheeseman, J. R.; Scalmani, G.; Barone, V.; Petersson, G. A.; Nakatsuji, H.; Li, X.; Caricato, M.; Marenich, A. V.; Bloino, J.; Janesko, B. G.; Gomperts, R.; Mennucci, B.; Hratchian, H. P.; Ortiz, J. V.; Izmaylov, A. F.; Sonnenberg, J. L.; Williams; Ding, F.; Lipparini, F.; Egidi, F.; Goings, J.; Peng, B.; Petrone, A.; Henderson, T.; Ranasinghe, D.; Zakrzewski, V. G.; Gao, J.; Rega, N.; Zheng, G.; Liang, W.; Hada, M.; Ehara, M.; Toyota, K.; Fukuda, R.; Hasegawa, J.; Ishida, M.; Nakajima, T.; Hon-da, Y.; Kitao, O.; Nakai, H.; Vreven, T.; Throssell, K.; Montgomery Jr., J. A.; Peralta, J. E.; Ogliaro, F.; Bearpark, M. J.; Heyd, J. J.; Brothers, E. N.; Kudin, K. N.; Staroverov, V. N.; Keith, T. A.; Kobayashi, R.; Normand, J.; Raghavachari, K.; Rendell, A. P.; Burant, J. C.; Iyengar, S. S.; Tomasi, J.; Cossi, M.; Millam, J. M.; Klene, M.; Adamo, C.; Cammi, R.; Ochterski, J. W.; Mar-tin, R. L.; Morokuma, K.; Farkas, O.; Foresman, J. B.; Fox, D. J. Gaussian 16 Rev. C.01; Wallingford, CT, 2016.

(10) Becke, A. D. Density-functional Thermochemistry. III. The Role of Exact Exchange. J. Chem. Phys. 1993, 98 (7), 5648–5652.

(11) Kendall, R. A.; Dunning, T. H.; Harrison, R. J. Electron Affinities of the First-row Atoms Revisited. Systematic Basis Sets and Wave Functions. J. Chem. Phys. 1992, 96 (9), 6796–6806.

(12) Woon, D. E.; Dunning, T. H. Gaussian Basis Sets for Use in Correlated Molecular Calculations. III. The Atoms Aluminum through Argon. J. Chem. Phys. 1993, 98 (2), 1358–1371.